JOC Article

Conformational Analysis of 2-Substituted Cyclobutane-α-amino Acid Derivatives. A Synergistic Experimental and Computational Study

Gonzalo Jiménez-Osés, Francisco Corzana, Jesús H. Busto, Marta Pérez-Fernández, Jesús M. Peregrina,* and Alberto Avenoza*

Departamento de Química, Universidad de La Rioja, Grupo de Síntesis Química de La Rioja, U.A.-C.S.I.C., 26006 Logroño, Spain

alberto.avenoza@dq.unirioja.es

Received October 21, 2005

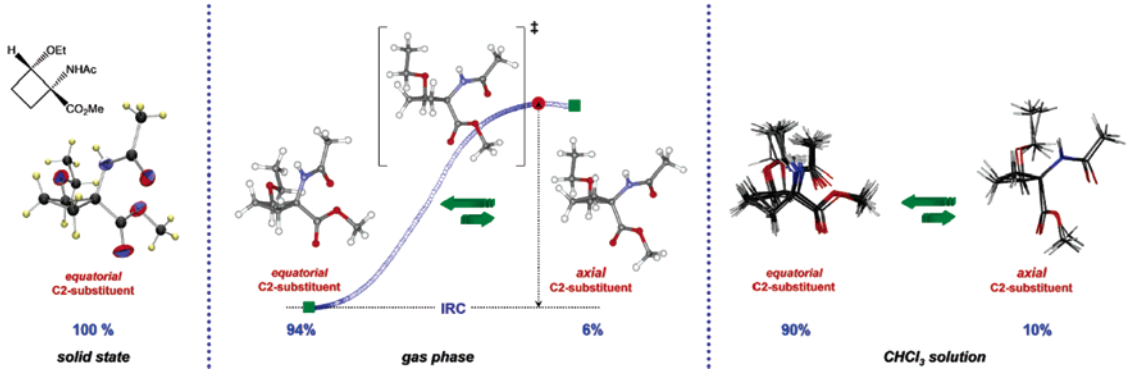

An extensive conformational study of different 2-substituted cyclobutane-α-amino acid derivatives in the solid state, in the gas phase, and in solution has been carried out. The study combines experimental techniques, such as X-ray diffraction and NMR spectroscopy, and computational methods, such as DFT calculations and molecular dynamics (MD) simulations, in a set solvent. The study reveals that the substituent at C2 in the cyclobutane ring, when fixed in an equatorial position, modulates the conformational preference of the ring-puckering.

Introduction

The conformational study of four-membered ring systems has attracted only a modest degree of attention in recent years, especially when compared to the five- or six-membered rings.[1] On the other hand, a recent book[2] and reviews[3] have reflected the great synthetic and structural interest that these small rings warrant. In addition, the small number of conformational studies on biomolecules with 1-aminocyclobutanecarboxylic acid residues revealed that this type of amino acid derivative promotes folded conformations when incorporated into both α- and β-peptides.[4]

As part of our global project on the synthesis and conformational study of glycopeptides, we recently synthesized cyclobutane serine analogues from methyl 2-acetamidoacrylate.[5] Additionally, several cyclobutane compounds were synthesized as intermediates in this synthetic path or in related syntheses.[6] Bearing in mind the importance that the conformational prefer-

* To whom correspondence should be addressed. Fax: +34 941 299655.

(1) (a) *Conformational Behavior of Six-Membered Rings*; Juaristi, E., Ed.; VCH Publishers: New York, 1995. (b) *The Conformational Analysis of Cyclohexenes, Cyclohexadienes, and Related Hydroaromatic Compounds*; Rabideau, P. W., Eds.; VCH Publishers: New York, 1989.

(2) *Patai Series: The Chemistry of Cyclobutanes*; Rapaport, Z., Liebman, J. F., Eds.; John Wiley & Sons: New York, 2005.

(3) (a) Namyslo, J. C.; Kaufmann, D. E. *Chem. Rev.* **2003**, *103*, 1485−1537. (b) Lee-Ruff, E.; Mladenova, G. *Chem. Rev.* **2003**, *103*, 1449−1483. (c) Avontis, F. *Russ. Chem. Rev.* **1993**, *62*, 897−906.

(4) (a) Balaji, V. N.; Ramnarayan, K.; Chan, M. F.; Rao, S. N. *Peptide Res.* **1995**, *8*, 178−186. (b) Gatos, M.; Formaggio, F.; Crisma, M.; Toniolo, C.; Bonora, G. M.; Benedetti, Z.; Di Blasco, B.; Iacovino, R.; Santini, A.; Saviano, M.; Kamphuis, J. *J. Pept. Sci.* **1997**, *9*, 110−122. (c) Izquierdo, S.; Kogan, M. J.; Parella, T.; Moglioni, A. G.; Branchadell, V.; Giralt, E.; Ortuño, R. M. *J. Org. Chem.* **2004**, *69*, 5093−5099.

(5) (a) Avenoza, A.; Busto, J. H.; Canal, N.; Peregrina, J. M. *Chem. Commun.* **2003**, 1376−1377. (b) Avenoza, A.; Busto, J. H.; Canal, N.; Peregrina, J. M. *J. Org. Chem.* **2005**, *70*, 330−333. (c) Avenoza, A.; Busto, J. H.; Canal, N.; Peregrina, J. M.; Pérez-Fernández, M. *Org. Lett.* **2005**, 3597−3600.

10.1021/jo0521955 CCC: $33.50
Published on Web 02/01/2006

SCHEME 1. Definition of the Pucker Angle with the Two Types of Subtituents at C2 (e = Equatorial and a = Axial).

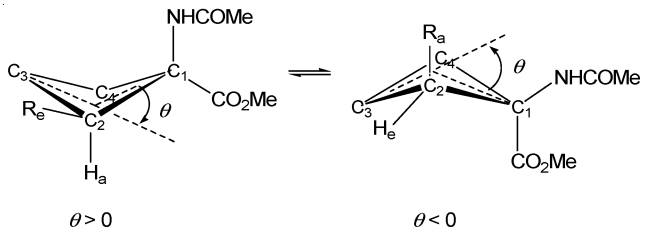

ences of these systems[4] could have when they are incorporated into model glycopeptides, we decided to carry out a conformational analysis of some selected 1,1,2-trisubstituted cyclobutane-rings as a first step in gaining a deeper understanding of these systems.

In this sense, the structure of cyclobutane raises some interesting questions. A four-membered ring can be either planar or puckered.[7] On one hand, the planar ring would have minimal angle strain, characterized by the C−C−C angles. On the other hand, it would have maximum torsional strain, characterized by the pucker angle θ, which is defined as the acute angle between the planes $C_1-C_2-C_4$ and $C_2-C_3-C_4$ (Scheme 1).

The puckering of the ring leads to a reduction in the torsional strain, but at the same time, the C−C−C bond angles are reduced, leading to increased bond angle strain. Thus, the equilibrium geometry is a result of the tension between these two strain terms.

As a result of the puckering in neat cyclobutane, two different dispositions of hydrogen atoms can be observed—equatorial and axial. This is similar to the situation in cyclohexane, and for this reason, monosubstituted derivatives can exist as axial or equatorial conformers. As in cyclohexyl compounds, the equatorial conformer is the most stable one and the inversion barriers ($\Delta E^{\ddagger}$) for monosubstituted cyclobutanes[3] are between 1.8 and 2.00 kcal·mol^{-1}, showing lower values than those observed in cyclohexanes.

It is clear that an understanding of the conformational preferences of four-membered rings is essential to study the effect that cyclobutane amino acids can have on the backbone and the lateral chains when incorporated into peptides and glycopeptides. However, in this field, the detailed geometry of 1,1,2-trisubstituted cyclobutanes is yet to be elucidated.[8]

For this reason, we have carried out an extensive study of the cyclobutane derivatives shown in Scheme 2 in the solid state, in the gas phase, and in $CHCl_3$ solution. The study focused on the conformational preferences of the four-membered ring as well as the energy involved in the inversion barrier associated with the two conformers of the ring. The study involved the use of computational tools, such as DFT and molecular dynamics simulations (DM) in a set solvent, and experimental techniques, such as X-ray diffraction and NMR measurements, which were used to validate the simulations.

Results and Discussion

Definitions and Target Compounds. As commented above, in recent papers we reported the synthesis of cyclobutane serine analogues, in which the key step in the synthetic pathway was the formal [2 + 2] cycloaddition (in the absence of catalyst) between methyl 2-acetamidoacrylate (**MAA**) and ketene diethyl acetal,[5a] which gave compound **1**. Compounds **2a** and **2s** were obtained from compound **1** through the key cyclobutanone intermediate (**CB**) and several other reactions (Scheme 2).[5b]

On the other hand, compounds **3a** and **3s** were synthesized through selective Michael-aldol reactions using sterically hindered aluminum aryloxides as Lewis acids; **3a** with methylaluminum bis-(4-bromo-2,6-di-*tert*-butyl phenoxide) (**MABR**) and **3s** using methylaluminoxane (**MAO**).[5c]

The new compounds **4a** and **4s** were prepared from the corresponding cyclobutanone **CB** using the route described in the literature,[6] but in this case with some minor modifications depicted in Scheme 2.

In summary, compounds **1**,[5a] **2s**,[5b] **2a**,[5b] **3s**,[5c] and **3a**[5c] were previously synthesized and compounds **4s** and **4a** have been synthesized in this study from cyclobutane derivatives with the aim of evaluating the stereoelectronic effect of the oxygen atom linked to C2 position of cyclobutane. The numbering and labeling scheme employed in this work for all compounds are shown in Scheme 2. The letters "s" and "a" refer to *syn* and *anti* stereoisomers with respect to the acetamide group, respectively.

Solid State. The crystal structures of **1**,[5a] **2s**,[8b] **2a**,[8b] and **3s**[5c] are shown in Figure 1. As can be seen, compound **1** presents two different structures (denoted as **A** and **B**) in the unit cell. From these results some important conclusions can be drawn with respect to the solid state. First, the substituent at C2 always occupies an equatorial position (compounds **2s**, **2a**, and **3s**), and as a consequence, the *anti* and *syn* derivatives adopt only one ring-puckering conformation, which is clearly opposite for each stereoisomer. Evidently, this trend disappears in the case of derivative **1**, in which both ring-puckering conformations place an ethoxy group in an equatorial position. This fact leads to the existence of both puckering conformers in the unit cell. Additionally, the *syn* compounds are stabilized by an intramolecular hydrogen bond between the NH of the amide and the oxygen of the ether group. Analysis of the C−C distances emphasizes the particularly long distance corresponding to C1−C2, 1.57 Å vs 1.55 Å found as an average measurement in similar structures,[8b] and the short distance for C2−C3, 1.52 Å vs 1.54 Å, and C3−C4, 1.52 Å vs 1.54 Å. On the other hand, the conformation adopted by the amido ester moiety is always the same, regardless of the ring-puckering and the relative position (*anti* or *syn*) of the substituent at C2. The aforementioned distances and the principal angles are summarized in Table 1 along with the $H_{4a}-H_{2a}$ distances for these structures, which were used as a starting point to perform the theoretical calculations and to validate these calculations.

Theoretical Studies in the Gas Phase. Minimum Energy Conformations. The aforementioned special features that govern the four-membered ring conformations led us to carry out an extensive theoretical study in order to evaluate the nature of the conformational differences in the related compounds. This investigation was performed in the gas phase in terms of the density functional theory (DFT) using the B3LYP hybrid functional[9] and the standard 6-31+G(d) basis set (see the

(6) Avenoza, A.; Busto, J. H.; Peregrina, J. M.; Pérez-Fernández, M. *Tetrahedron* **2005**, *61*, 4165−4172.

(7) *Stereochemistry of Organic Compounds*; Eliel, E. L., Wilen, S. H., Eds.; John Wiley & Sons: New York, 1994.

(8) (a) Hittich, R. *Org. Magn. Reson.* **1982**, *18*, 214−218. (b) Avenoza, A., Busto, J. H., Canal, N., Peregrina, J. M. Structural analysis of acetamidocyclobutanes by a combination of X-ray diffraction and NMR spectroscopy. In *Structural Analysis of Cyclic Systems*; Iriepa, I., Ed.; Research Signpost, T. C.: India, 2005; pp 55−68.

SCHEME 2. Schematic Representation of All of the Compounds Studied and Their Synthetic Routes[a]

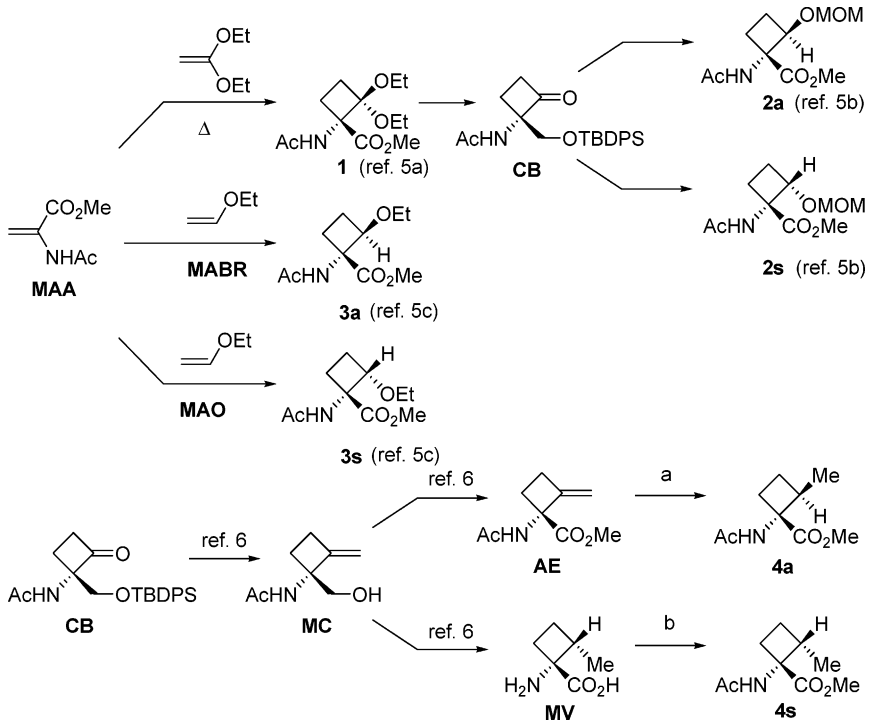

[a] Reagents and conditions: (a) H_2, Pd/C, CH_2Cl_2, rt, 15 h, 87%; (b) (i) AcCl, MeOH, rt, 1 h, (ii) Ac_2O, pyridine, rt, 1 h, 81%.

TABLE 1. Comparison of the Parameters Obtained for Different Structures (Distances Are Reported in Å, Angles in Degrees)

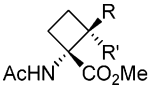

1: R = R' = OEt
2a: R = OMOM, R' = H
2s: R = H, R' = OMOM
3s: R = H, R' = OEt

	structures				
parameters	**1A**	**1B**	**2s**	**2a**	**3s**
C_1-C_2	1.57	1.58	1.56	1.56	1.57
C_2-C_3	1.54	1.54	1.52	1.52	1.52
C_3-C_4	1.52	1.51	1.53	1.52	1.52
C_4-C_1	1.54	1.55	1.55	1.54	1.54
$C_1-C_2-C_3$	88.5	88.7	89.1	89.2	88.5
$C_2-C_3-C_4$	88.2	89.1	88.6	88.8	88.8
$C_3-C_4-C_1$	90.2	90.1	90.0	89.5	89.7
$C_4-C_1-C_2$	86.6	86.3	86.3	86.6	86.2
θ	+26.8	−23.6	+28.0	−25.6	+27.6
$H_{4a}-H_{2a}$	−	−	2.81	2.84	2.70

TABLE 2. Calculated Energies (kcal·mol^{-1}), Entropies (cal·mol^{-1}·K^{-1}), and Gibbs Free Energies (kcal·mol^{-1}) of the Minima and Transition Structures [B3LYP/6-31+G(d)-Optimized Geometries]

structures	$\Delta\Delta E^a$	S[a]	$\Delta\Delta G_{298}{}^a$	$\Delta\Delta G^b$
1A	0.13	152.9	0.17	0.30
1B	0.00	153.5	0.00	0.00
TS_1	1.55	147.5	1.20	2.75
3s_eq	0.00	134.5	0.00	0.00
3s_ax	2.13	135.8	−0.47	1.66
TS_3s	2.17	131.2	0.30	2.47
3a_eq	0.00	134.8	0.00	0.00
4s_eq	0.00	120.8	0.00	0.00
4s_ax	0.95	122.0	−0.42	0.53
TS_4s	1.11	117.4	0.40	1.51
4a_eq	0.00	121.4	0.00	0.00
4a_ax	1.10	121.4	0.07	1.17
TS_4a	1.25	117.3	0.63	1.88

[a] Calculated at the B3LYP/6-31+G(d) level. [b] Calculated with $\Delta\Delta G = \Delta\Delta E + \Delta\Delta G_{298}$.

Computational Details). We based our study on the assumption that the energy barrier associated with the ring inversion of cyclobutanes can be theoretically calculated, leading to double-minimum ring-puckering potentials. The difference in energy between these two minima gives a quantitative idea of the preferred ring conformation. With this aim in mind, the whole conformational space of compounds **1**, **3s**, **3a**, **4s**, and **4a** was initially explored. Methoxymethyl ether derivatives **2s** and **2a** were not included in the study due to their structural equivalence with **3s** and **3a**. The structures and relative energies calculated for the minimum energy conformers of all compounds are summarized in Table 2 and Figures 2 and 3. The notation used for the conformers involves adding the terms "eq" or "ax" to the compound number. These terms indicate that the substituent at C2 is situated in an equatorial or axial position, respectively. The ring-puckering angles θ are shown for comparison with the solid-state values.

In summary, and from the geometric point of view, good agreement was obtained between the calculated structures and the available crystal structures, with differences between the experimental and the computed ring-puckering angles θ of only 1−2°. It is important to mention that only global minima for each ring-puckering conformation were considered for discussion, and therefore, some minor conformational changes can be observed from one ring conformer to another.

In the case of 2,2-disubstituted cyclobutane **1**, two ring-puckering conformers (**1A** and **1B**) were found, a situation in total agreement with the crystallographic findings. The differ-

(9) (a) Lee, C.; Yang, W.; Parr, R. *Phys. Rev. B* **1988**, *37*, 785−789. (b) Becke, A. D. *J. Chem. Phys.* **1993**, *98*, 5648−5652.

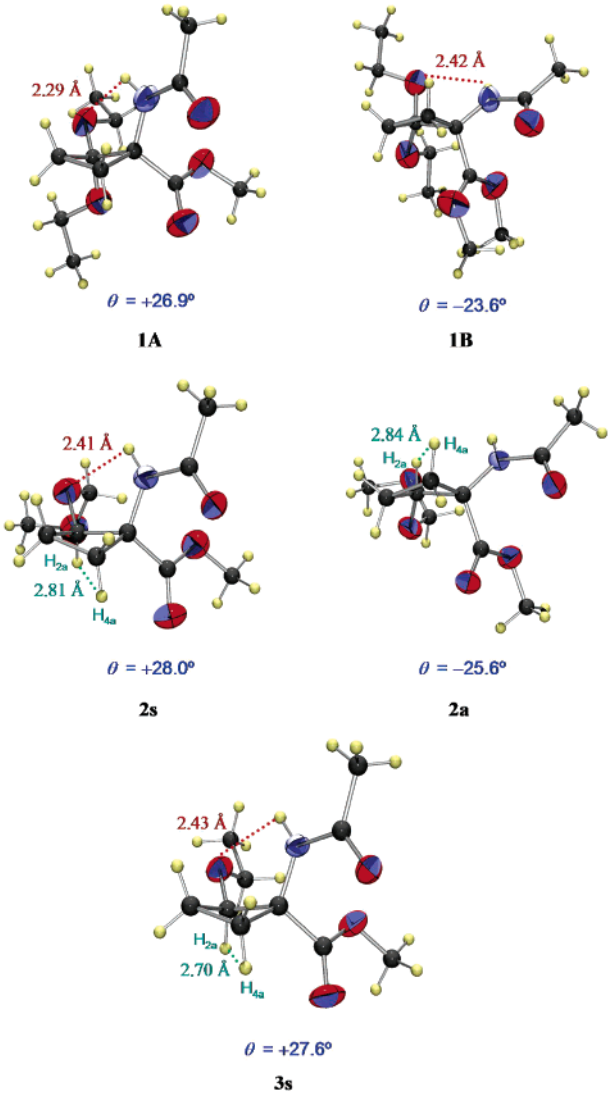

FIGURE 1. Some geometrical features of the crystal structures of cyclobutanes **1**, **2s**, **2a**, and **3s**. The H_{4a}−H_{2a} distance is labeled in green and the NH···O distance in red.

ence in energy between these structures is only 0.30 kcal·mol^{-1}. In contrast, only one single ring-puckering conformer (**3a_eq**) could be located for compound **3a**. In the case of compound **3s**, although the two possible ring-puckering conformers were found, the one in which the ethoxy group is equatorial (**3s_eq**) was considerably more favorable (by 1.66 kcal·mol^{-1}) than the other (**3s_ax**). Interestingly, both conformers of derivative **3s** are stabilized by an intramolecular hydrogen bond between the amide and the ether groups (Figure 2), with the NH···O distance even shorter in the case of the less stable structure **3s_ax**. This finding led us to consider this interaction as a nondeterminant factor in the conformational preferences and made it necessary to evaluate other stabilizing factors.

This high preference for one of the ring-puckering conformations decreases when the ethoxy group is replaced with a methyl group. In this case, the two possible ring-puckering conformations were located. For compound **4s**, the difference in energy between the two puckering conformations **4s_ax** and **4s_eq** was only 0.53 kcal·mol^{-1} in favor of **4s_eq**. However, this energetic difference for conformers **4a_ax** and **4a_eq** was significantly

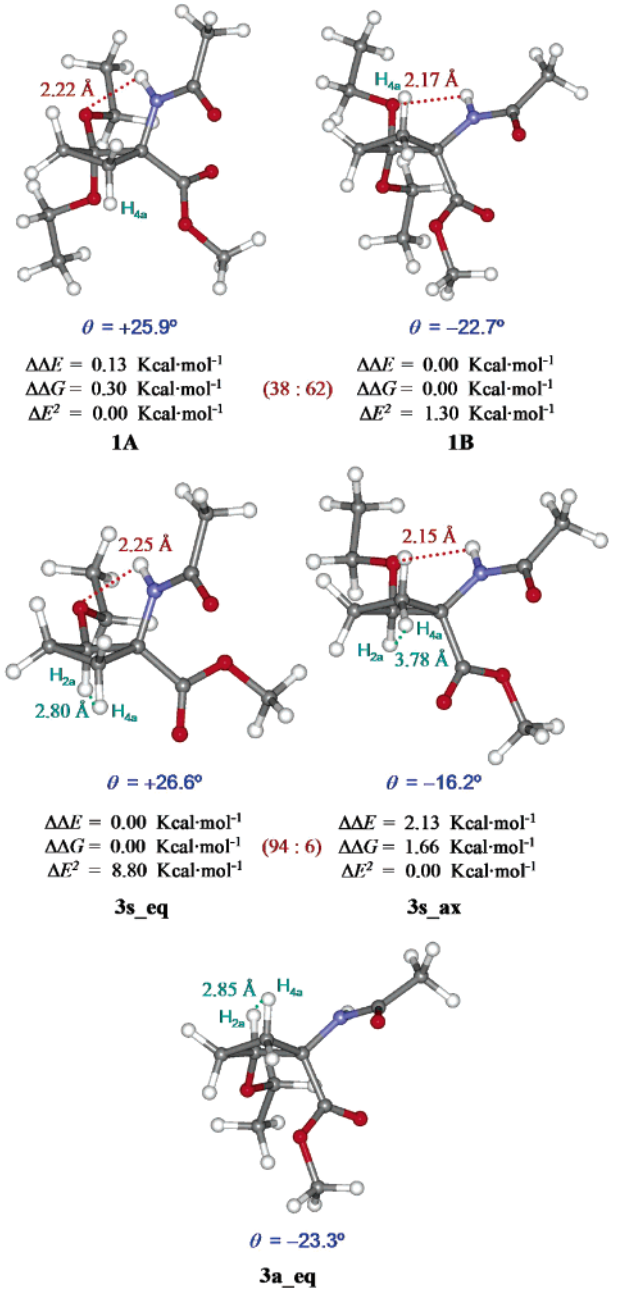

FIGURE 2. 3D-representations of the fully optimized B3LYP/6-31G+(d) global minima for compounds **1**, **3s**, and **3a**. H_{4a}−H_{2a} distances are labeled in green and NH···O distances in red. The relative population of each ring-puckering conformer is given in parentheses. ΔE^2 is the relative second-order perturbation energy estimated for all hyperconjugative interactions present within the four-membered ring.

higher in compound **4a**, with the conformer **4a_eq** being 1.17 kcal·mol^{-1} more stable (Figure 3).

The relative Gibbs free energies of the minimum of each ring-puckering conformer ($\Delta\Delta G$) were used to estimate the relative population from a Maxwell−Boltzmann distribution at 273 K (see Figures 2 and 3).

One important conclusion emerges from considering both the solid state and the calculated gas-phase structures: the *syn* or *anti* orientation of the substituent at C2 plays a key role in determining the ring conformation. In this way, when this substituent has a *syn* orientation with respect to the acetamide group, the cyclobutane ring puckers preferentially to positive θ

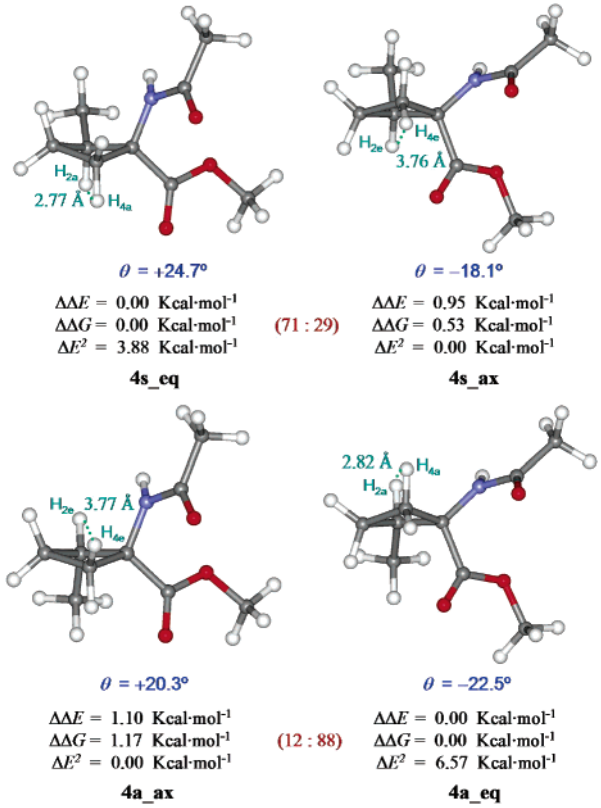

FIGURE 3. 3D-representations of the fully optimized B3LYP/6-31G+(d) global minima for compounds **4s** and **4a**. $H_{4a}-H_{2a}$ and $H_{4e}-H_{2e}$ distances are labeled in green. The relative population of each ring-puckering conformer is given in parentheses. ΔE^2 is the relative second-order perturbation energy estimated for all hyperconjugative interactions present within the four-membered ring.

values, but when these groups are placed in an *anti* arrangement, the most stable conformers always show negative θ values. This feature makes the substituent at C2 adopt an equatorial position in all cases.

Transition Structures. In the cases where the two ring-puckering conformations were found (**1**, **3s**, **4s**, and **4a**), the ring-puckering surfaces were completely examined through relaxed potential energy surface (PES) scans and intrinsic reaction coordinate (IRC) calculations,[10] with almost identical results obtained with both methodologies. As an example, two IRC calculations for **3s** and **4s** are shown in Figure 4a. As can be seen, the IRC calculations connect two local minima of the whole electronic energy ($\Delta\Delta E$) surface through a single transition structure (**TS_3s** and **TS_4s**, respectively). In contrast to the symmetric double-minimum ring-puckering potentials calculated for unsubstituted cyclobutane,[11] the transition structures are very similar in energy and, consequently, in geometry to their respective less stable minima. The geometries and relative energies of all the transition structures calculated using the aforementioned procedures are shown in Figure 4b: **TS_1**, **TS_3s**, **TS_4s** and **TS_4a**. It can be seen that the activation barriers are higher in **1** and **3s**, with relative energy values of 2.75 and 2.47 kcal·mol^{-1}, respectively. Interestingly, these values are higher than those for monosubsituted cyclobutanes.[2]

(10) (a) Fukui, K. *J. Phys. Chem.* **1970**, *74*, 4161−4163. (b) Fukui, K. *Acc. Chem. Res.* **1981**, *14*, 363−368.

(11) Glendening, E. D.; Halpern, A. M. *J. Phys. Chem. A* **2005**, *109*, 635−642.

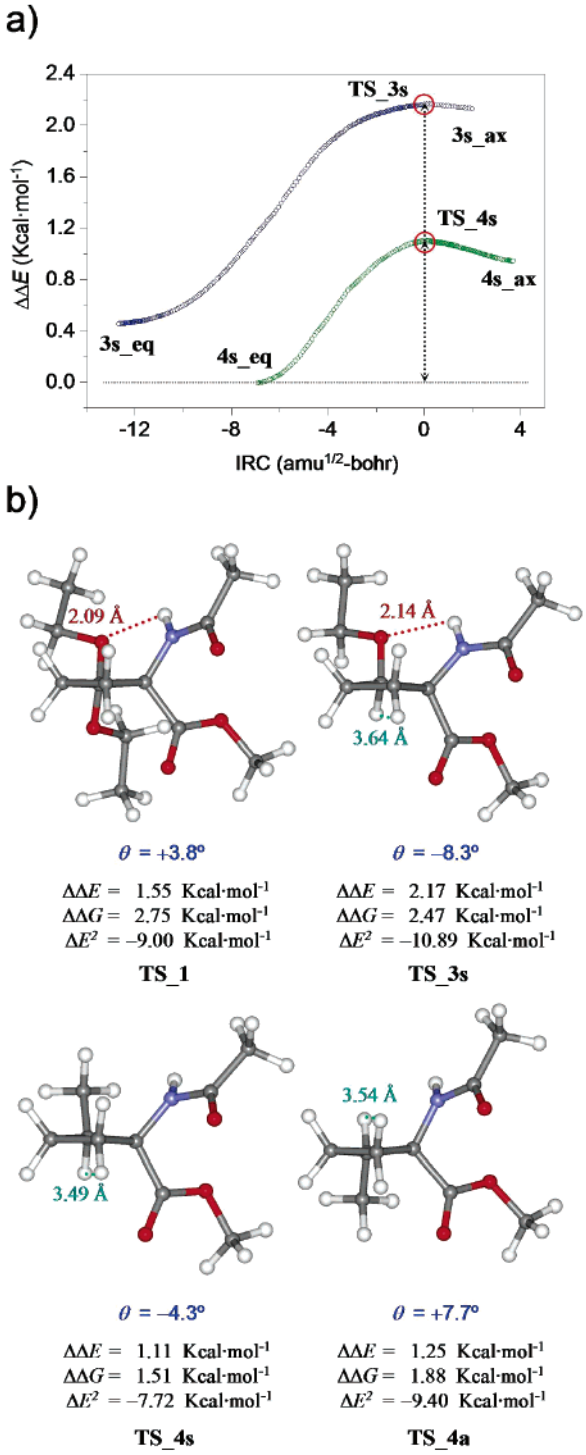

FIGURE 4. (a) IRC calculations for **3s** and **4s**. (b) Transition structures and relative energies for the respective global minima calculated for **TS_1**, **TS_3s**, **TS_4s**, and **TS_4a**. All calculations were carried out at the B3LYP/6-31+G(d) level. H_4-H_2 distances are labeled in green and NH···O distances in red. ΔE^2 is the relative second-order perturbation energy estimated for all hyperconjugative interactions present within the four-membered ring.

This result can be explained by assuming, among other factors discussed below, higher steric requirements for the ether group-(s) in the planar form in comparison to the methyl group. Thus, compounds **4s** and **4a** are expected to be more flexible on the basis of the lower activation energy calculated for their ring

TABLE 3. Detailed Second-Order Perturbation Energies (kcal·mol^{-1}) Estimated for the Minima and Transition Structures through Natural Bond Orbital (NBO) Analysis [B3LYP/6-31+G(d)-Optimized Geometries]

structures	$\sigma_{CC}\rightarrow\sigma_{CR}^*$	$\sigma_{CR}\rightarrow\sigma_{CC}^*$	$\sigma_{CR}\rightarrow\sigma_{CR}^*$	$n_O\rightarrow\sigma_{CR}^*$	$n_O\rightarrow\sigma_{CC}^*$	$n_N\rightarrow\sigma_{CR}^*$	$n_N\rightarrow\sigma_{CC}^*$	E^2	ΔE^2
1A	26.08	1.37	20.97	30.02	23.54	7.17	6.03	115.18	0.00
1B	26.49	1.21	20.56	29.76	23.99	5.76	8.71	116.48	1.30
TS_1	20.29	0.54	19.02	29.31	24.03	7.69	6.60	107.48	−9.00
3s_eq	24.89	1.43	19.94	6.56	14.08	8.59	6.09	81.58	8.80
3s_ax	20.75	0.76	18.92	6.39	10.93	6.48	8.55	72.78	0.00
TS_3s	19.04	0.49	18.59	6.44	11.23	7.28	7.62	70.69	−10.89
3a_eq	26.20	0.65	20.76	7.28	14.82	9.10	3.63	82.44	0.00
4s_eq	23.15	1.32	20.23			9.24	3.94	57.88	3.88
4s_ax	21.40	0.79	17.98			9.19	4.64	54.00	0.00
TS_4s	18.52	0.34	17.83			9.14	4.33	50.16	−7.72
4a_eq	24.58	1.09	19.33			9.24	4.84	59.08	6.57
4a_ax	19.95	0.95	18.73			8.73	4.15	52.51	0.00
TS_4a	18.05	0.45	18.18			8.78	4.22	49.68	−9.40

inversion (less than 2 kcal·mol^{-1} in both cases), which makes them more similar to the monosubstituted systems.[2]

The expected small values obtained for all of the activation barriers (1−3 kcal·mol^{-1})[2] make the ring inversion possible even at very low temperatures, so that the conformational preferences observed must be necessarily explained in terms of relative stability of each ring-puckering conformer. However, and, according to Glendening et al.,[11] the numerical values of these barriers are not a decisive feature in the context of this work, and could be somewhat inexact when they are calculated with a non highly correlated method without basis set extrapolation, such as B3LYP/6-31+G(d) method.

Stabilizing Interactions. As discussed above, there is a clear conformational preference for the ring-puckering conformer that situates the substituent at C2 in an equatorial position. Although this finding can be easily explained in terms of steric factors, we decided to study other less explored features, such as hyperconjugation, to explain the observed conformational tendencies. In this sense, Glendening et al.[11] recently demonstrated the important role that hyperconjugation plays in the inversion barrier of cyclobutane, with the equatorial $\sigma_{CC}\rightarrow\sigma_{CH}^*$ and the axial-axial $\sigma_{CH}\rightarrow\sigma_{CH}^*$ donor−acceptor interactions being the major causes of the puckered geometries. This kind of hyperconjugative interaction is usually examined through natural bond orbital (NBO) analysis[12] and can help in evaluating the relative stability of each ring conformation. The more complex construction of our derivatives led us to carry out a systematic analysis of all $\sigma_{CC}\rightarrow\sigma_{CR}^*$, $\sigma_{CR}\rightarrow\sigma_{CC}^*$, $\sigma_{CR}\rightarrow\sigma_{CR}^*$, $n_O\rightarrow\sigma_{CR}^*$, $n_O\rightarrow\sigma_{CC}^*$, $n_N\rightarrow\sigma_{CR}^*$, and $n_N\rightarrow\sigma_{CC}^*$ hyperconjugative interactions existing within the cyclobutane structures, including the related TS. It is worth commenting that all C−C antibonding and N and O (ether) lone pair orbitals must be included in the study due to the particular hyperconjugative capability of the cyclobutane substituents. The energies corresponding to these interactions, denoted as E^2, were estimated in terms of second-order perturbation theory analyses of Fock matrixes in NBO basis. Relative hyperconjugation energies (ΔE^2) are gathered in Figures 2−4 and Table 3. It is worth noting that relative hyperconjugation (ΔE^2) is more related to relative electronic energy ($\Delta\Delta E$) than to relative Gibbs free energy ($\Delta\Delta G$).

Hyperconjugative interactions are weakened by 8−11 kcal·mol^{-1} in the TS structures when compared to the corresponding global minima. Moreover, high inversion barriers are associated with the more important loss of this stabilizing energy. These differences in E^2 become smaller between each TS, and the correspondingly less stable minimum (2−4 kcal·mol^{-1}) is due to the aforementioned high similarity in energy and geometry.

As far as the minima are concerned, this stabilizing energy is considerably higher for the global minimum of each compound—with the exception of **1**, in which this conformational preference disappears and hyperconjugation has nearly the same value. Interestingly, relative hyperconjugations are greater when the differences in energy between the minima increase. In this sense, the sum of all E^2 values is 8.80 kcal·mol^{-1} higher for the most stable ring-puckering of **3s** (**3s_eq**) than for the other one (**3s_ax**). In contrast, for compounds **4s** and **4a**, for which the conformational preferences are lower, the differences in the sum of all E^2 are only 3.88 and 6.57 kcal·mol^{-1} and are always in favor of the most stable ring-puckered conformers **4s_eq** and **4a_eq**, respectively. Moreover, this difference in E^2 is only 1.30 kcal·mol^{-1} for **1**, in which no significant conformational preference exists. Therefore, although the observed conformational preferences for these compounds can be explained in terms of steric factors alone, it is important to stress that hyperconjugative interactions, which are maximum when the substituent at C2 is placed in an equatorial position, could also play an important role.

Conformational Analysis in Solution. The structures of compounds **3s**, **3a**, **4s**, and **4a** in solution were determined by combining NMR experiments and MD simulations. In the first step, selective 1D-NOESY experiments were carried out at 293 K and 400 MHz. The experimentally determined distances between H_{2a} and H_{4a} for compounds **4s** and **4a** were easily derived from the corresponding NOE build-up curves,[13] using the fixed distance $H_{4a}-H_{4e}$ as a reference (Figure 5). For compounds **3s** and **3a**, the average $H_{4a}-H_{2a}$ distance (r) could be estimated using the ISPA method,[14] considering the absolute integrals of the cross-peak volume of $H_{4a}-H_{4e}$ as a reference (I_{ref}) and the cross-peak volume of $H_{4a}-H_{2a}$ (I). Equation 1 was applied.

$$r = r_{ref}(I_{ref}/I)^{1/6} \quad (1)$$

Interestingly, the average $H_{4a}-H_{2a}$ distances are related to the ring-puckering family or families adopted by the four-

(12) (a) Reed, A. E.; Curtiss, L. A.; Weinhold, F. *Chem. Rev.* **1988**, *88*, 899−926. (b) NBO 5.0: Glendening, E. D.; Badenhoop, J. K.; Reed, A. E.; Carpenter, J. E.; Bohmann, J. A.; Morales, C. M.; Weinhold, F. Theoretical Chemistry Institute, University of Wisconsin: Madison, WI, 2001.

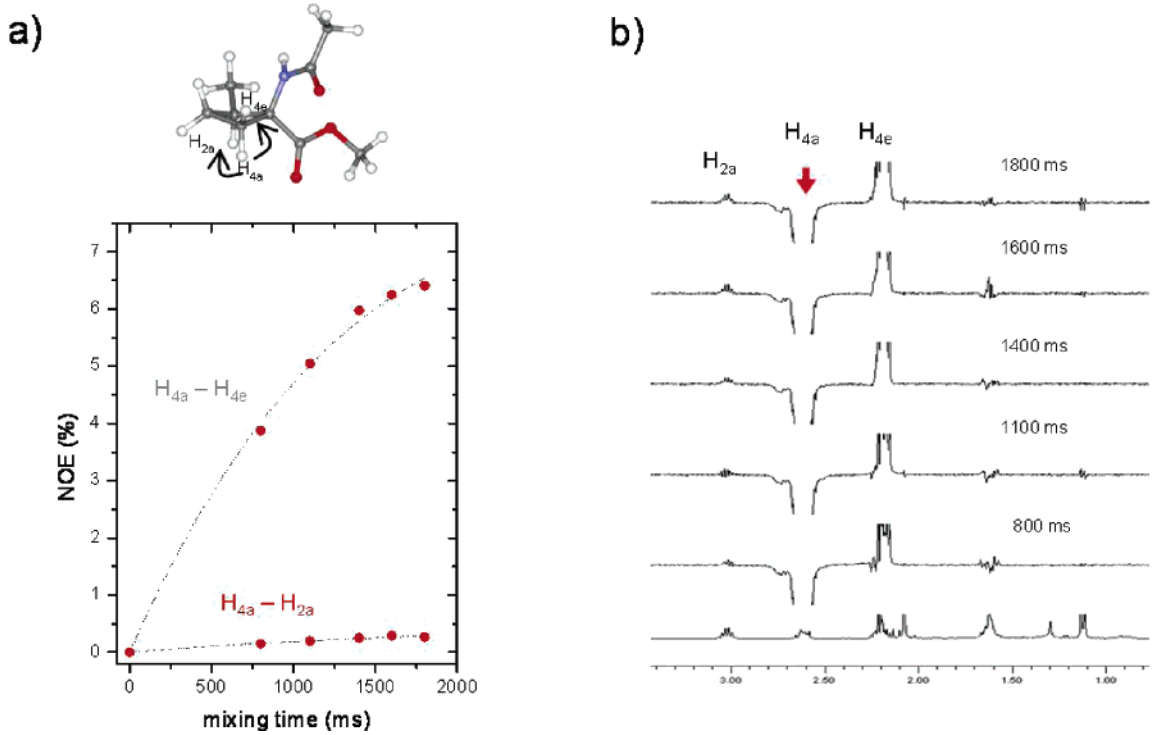

FIGURE 5. (a) (Top) Schematic representation of the experimental information employed in the structural analysis of **4s**. (Bottom) NOE build-up curves for compound **4s**. NOE corresponding to known fixed distances employed as a reference are labeled in gray. NOE corresponding to unknown distances are labeled in red. (b) Selective 1D-NOESY experiments with the 1D-DPFGSE NOE pulse sequence, corresponding to the inversion of H_{4a} in compound **4s** at different mixing times.

TABLE 4. Experimental and Theoretical (H_{4a}−H_{2a}) Distances Obtained for Compounds 3a, 3s, 4a and 4s

	$d(H_{4a}-H_{2a})$ (Å)	
compound	expt	MD-tar
3s	2.8	3.0
3a	2.7	2.9
4s	3.1	2.9
4a	2.9	3.0

membered ring in solution. Thus, to obtain an experimentally derived ensemble, 4 ns MD-tar (molecular dynamics with time-averaged restrains)[15] simulations were carried out using a set solvent ($CHCl_3$) by inclusion of these experimental distances (H_{4a}−H_{2a}) as time-averaged restraints. This simulation was carried out using the AMBER 6.0 program[16] implemented with the latest and general AMBER force field[17] (GAFF). In this sense, although this force field has been specifically designed to cover most organic molecules, care must be taken in its use and the results obtained from the simulations must be considered only from a qualitative point of view.

The relevant NOE-derived distances H_{4a}−H_{2a} are shown in Table 4 together with those obtained from MD-tar simulations. As can be seen, the trajectories obtained were able to reproduce the experimental data quite well.

According to MD simulations, cyclobutanes **3s**, and in particular **3a**, are quite rigid and present one major conformer in solution. This conformer is similar in geometry to that obtained in the gas phase (**3s_eq** and **3s_ax**), with θ dihedral angles of around +44° and −33°, respectively. The ensembles obtained for conformers of **3a** and **3s** that reproduce the experimental data are shown in Figure 6 along with the θ angle distributions. In the case of **3s**, the minor conformation has a relative population of 10% and a θ value of about −12°. Both conformers have an intramolecular hydrogen bond between NH···O, which is present at a level of about 71% of the total trajectory time (distance NH···O < 2.5 Å).

In contrast, our NMR/MD approach indicates that derivatives **4s** and **4a** exhibit a significant degree of flexibility (Figure 6). This fact is corroborated by the larger average H_{4a}−H_{2a} distances obtained by NMR spectroscopy in comparison to those in the 2-ethoxy-substituted derivatives. Compound **4s** presents two different puckering arrangements and these are characterized by θ angles of −22° and +43° and relative populations of 36:64, respectively. A similar situation was obtained for **4a**, with two major families characterized by θ angles of −25° and +41° and relative populations of 80:20, respectively. It must be stressed that, although the force field seems to overestimate the θ values, the results obtained in this work for the solution state are qualitatively in good agreement with the DFT calculations in the gas phase. As expected, in all cases the main conformer in $CHCl_3$ solution has the substituent at C2 in an equatorial disposition. Logically, apart from inversional flexibility of cyclobutane ring, the considered compounds also possess torsional flexibility of the substituent groups, as it is shown in Supporting Information. In particular, the ester and amide groups mainly adopt the same orientation as that predicted by the DFT

(13) For a recent example of NOE buildup curves, see: Haselhorst, T.; Weimar, T.; Peters, T. *J. Am. Chem. Soc.* **2001**, *123*, 10705−10714.
(14) Woods, R. J.; Pathiaseril, A.; Wormald, M. R.; Edge, C. J.; Dwek, R. A. *Eur. J. Biochem.* **1998**, *258*, 372−386.
(15) Pearlman, D. A. *J. Biomol. NMR* **1994**, *4*, 1−16.
(16) Pearlman, D. A.; Case, D. A.; Caldwell, J. W.; Ross, W. S.; Cheatham, T. E.; DeBolt, S.; Ferguson, D.; Siebal, G.; Kollman, P. *Comput. Phys. Commun.* **1995**, *91*, 1−41.
(17) Wang, J.; Wolf, R. M.; Caldwell, J. W.; Kollman, P. A.; Case, D. A. *J. Comput. Chem.* **2004**, *25*, 1157−1173.

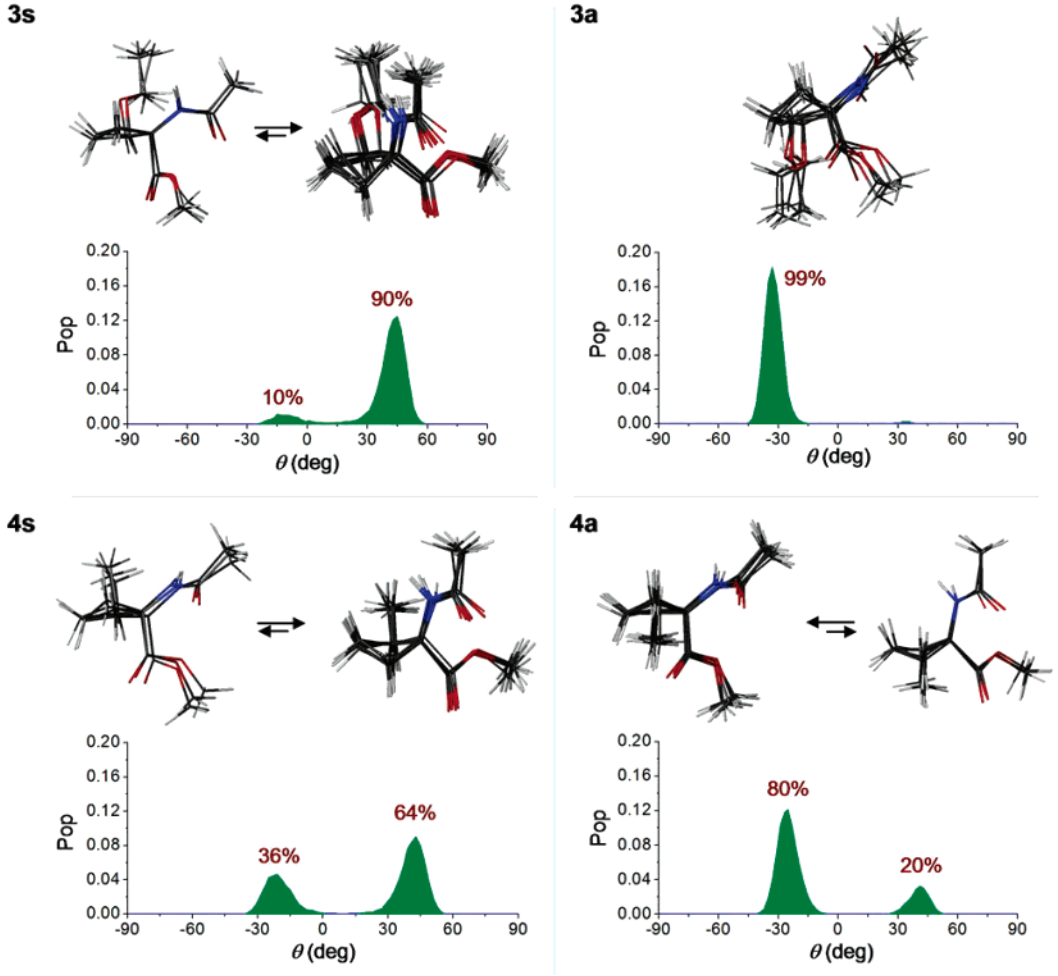

FIGURE 6. MD-tar ensembles and MD-tar θ dihedral distributions for compounds **3s**, **3a**, **4s**, and **4a**.

calculations in all the derivatives—the exception being **3a**, in which more flexibility is observed (Figure 6).

Finally, bearing in mind the importance of the average H_{4a}–H_{2a} distance to evaluate the ring-puckering in 1,1,2-trisubstituted cyclobutanes, we correlated the % population of the major conformer (from MD-tar) with the experimental distance extracted from NMR data (NOE). This correlation showed a linear relation, as can be seen from Figure 7 and the following equation.

$$\text{Pop}\ (\%) = 335.43 - 87.71 \times d(H_{4a} - H_{2a})$$
$$r = 0.999 \quad r^2 = 0.9977 \quad (2)$$

It is clear that distances shorter than 2.68 Å involve 100% of a single conformer, at least for this kind of 2-substituted cyclobutane-α-amino acid derivatives. Interestingly, eq 2 will provide a useful tool to analyze the population distribution taking into account the experimental values from NMR data.

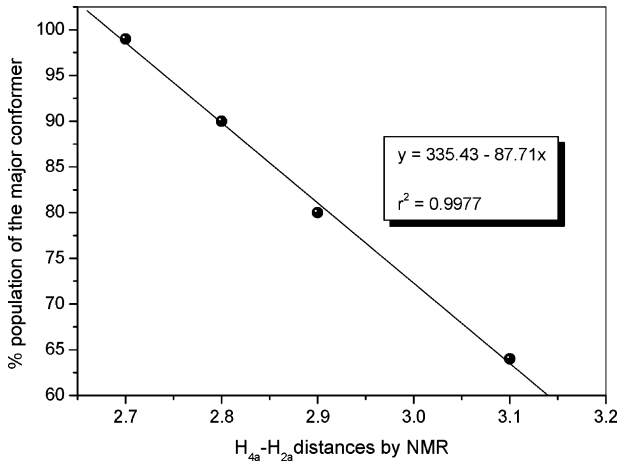

FIGURE 7. Relation between NMR data and MD-tar results.

Conclusions

To study the conformational preferences of the ring-puckering in cyclobutanes, an in-depth conformational analysis of different 2-substituted cyclobutane-α-amino acid derivatives has been carried out in the solid state, gas phase, and solution. Different techniques such as X-ray diffraction, NMR spectroscopy, DFT calculations, and MD simulations were combined in this study. The most important conclusions are summarized in the following paragraphs.

In the solid state, it was observed in the X-ray structures of cyclobutanes with one substituent at C2 that this one always occupies an equatorial position (compounds **2s**, **2a**, and **3s**). As a consequence, the *anti* derivative (**2a**) adopts only one ring-puckering conformation characterized by a negative pucker angle θ, while the unique ring-puckering conformation observed in

the *syn* derivatives (**2s** and **3s**) adopts positive pucker angles θ. This tendency disappears in the case of cyclobutane derivative **1** (two substituents at C2), in which both ring-puckering conformations are observed, with one ethoxy group in an equatorial position.

The aforementioned experimentally observed feature in the solid state was qualitatively reproduced in the DFT calculations made in the gas phase; the ring-puckering conformation that places the substituent at C2 in an equatorial position is the most stable for each compound studied, regardless of the nature of the substituent. Moreover, in several cases the ring-puckering surfaces were completely examined (IRC), locating the corresponding transition structures, and the activation barriers for the interconversion of the ring-puckering conformations of cyclobutane were estimated. In an effort to explain, without considering steric factors alone, why the substituent at C2 is preferentially situated in equatorial position -forcing a determined ring-puckering conformation- the role played by hyperconjugation in the inversion barrier of cyclobutane ring was examined. In conclusion, the stabilizing hyperconjugative interactions, which are maximum when the substituent at C2 is placed in an equatorial position, could also play an important role.

In solution, NMR experiments and MD simulations were performed on derivatives **3s**, **3a**, **4s**, and **4a**, and these once more showed the same characteristics as discussed above for gas phase and solid-state studies; the equatorial disposition of the substituent at C2 forces the ring-puckering conformations of the cyclobutane ring. Moreover, we found that the average $H_{4a}-H_{2a}$ distance (experimentally extracted from NOE data) in these cyclobutanes shows a linear relationship with the percentage of the population of the major conformer (deduced from MD simulations). Consequently, the corresponding equation could be used to estimate the population distribution of ring-puckering conformers of other 1,1,2-trisubstituted cyclobutanes in solution.

It can be concluded that, in the solid state, gas phase, and solution, the *syn* or *anti* orientation of the substituent at C2 with respect to the acetamide group plays a key role in the ring-puckering conformation of the 2-substituted cyclobutane-α-amino acid derivatives studied. In this way, the cyclobutane ring puckers preferentially to positive θ values in the *syn* derivatives, and the most stable conformers always show negative θ values in the *anti* derivatives.

Experimental Section

Synthetic Procedures. (1*R,2*R**)-1-Acetamido-2-methylcyclobutane-1-carboxylic Acid Methyl Ester (4a).** Palladium on carbon (1:10 catalyst/substrate by weight) was added to a solution of 1-acetamido-2-methylenecyclobutane-1-carboxylic acid methyl ester[6] (16 mg, 0.087 mmol) in dichloromethane (5 mL). The suspension was stirred under H_2 (1 atm) at room temperature for 15 h, and the catalyst was filtered off. The solvent was evaporated to give (1*R**,2*R**)-1-acetamido-2-methylcyclobutane-1-carboxylic acid methyl ester as a white solid. The compound was purified by silica gel column chromatography using EtOAc/MeOH (9:1) to give 14 mg of **4a** (87%). ^{1}H NMR ($CDCl_3$, 400 MHz): δ 0.99 (d, 3H, $J = 7.0$, CH_3), 1.65−1.81 (m, 1H, H_{3a}), 1.99 (s, 3H, $COCH_3$), 2.00−2.10 (m, 1H, H_{3e}), 2.11−2.24 (m, 1H, H_{4a}), 2.69−2.75 (m, 1H, H_{2a}), 2.76−2.84 (m, 1H, H_{4e}), 3.77 (s, 3H, CO_2CH_3), 6.14 (br s, 1H). ^{13}C NMR ($CDCl_3$, 100 MHz): δ 16.1, 23.3, 28.7, 29.3, 39.1, 52.0, 62.8, 169.8, 172.5. Anal. Calcd for $C_9H_{15}NO_3$: C, 58.36; H, 8.16; N, 7.56. Found: C, 58.65; H, 8.24; N, 7.63. The assignments were made by COSY, HSQC, and NOESY experiments.

(1*R,2*S**)-1-Acetamido-2-methylcyclobutane-1-carboxylic Acid Methyl Ester (4s).** The white solid (1*R**,2*S**)-1-amino-2-methylcyclobutane-1-carboxylic acid[6] (13 mg, 0.076 mmol) was dissolved into a solution of HCl/MeOH, prepared by dropwise addition of AcCl (50 μL, 0.23 mmol) to MeOH (3 mL) at 0 °C, and the mixture was stirred at room temperature for 1 h and then concentrated. The crude product was used in the next step without further purification. This compound was dissolved in pyridine (2 mL), and Ac_2O (1 mL) was added at room temperature and the mixture stirred for 1 h. The solvent was removed, and the crude product was purified by silica gel column chromatography using EtOAc/MeOH (9:1) to give 11 mg of **4s** (81%). ^{1}H NMR ($CDCl_3$, 400 MHz): δ 1.08 (d, 3H, $J = 7.2$, CH_3), 1.53−1.64 (m, 1H, H_{3a}), 2.03 (s, 3H, $COCH_3$), 2.07−2.21 (m, 2H, H_{3e}, H_{4e}), 2.50−2.61 (m, 1H, H_{4a}), 2.91−3.03 (m, 1H, H_{2a}), 3.74 (s, 3H, CO_2CH_3), 5.86 (br s, 1H). ^{13}C NMR ($CDCl_3$, 100 MHz): δ 15.4, 22.9, 23.7, 28.7, 36.0, 52.4, 60.4, 170.1, 173.7. Anal. Calcd for $C_9H_{15}NO_3$: C, 58.36; H, 8.16; N, 7.56. Found: C, 58.28; H, 8.12; N, 7.64. The assignments were made by COSY, HSQC, and NOESY experiments.

NMR Experiments. NMR experiments were carried out on a 400 MHz (^{1}H) spectrometer at 293 K. Selective 1D NOESY experiments were recorded employing the 1D-DPFGSE NOESY pulse sequence. NOE intensities were normalized with respect to the diagonal peak at zero mixing time. Experimental NOEs were fitted to a double-exponential function, $f(t) = \mathrm{p0}(e^{-\mathrm{p1}t})(1 - e^{-\mathrm{p2}t})$ with p0, p1, and p2 being adjustable parameters.[13] The initial scope was determined from the first derivative at time $t = 0$, $f'(0) = \mathrm{p0}\cdot\mathrm{p2}$. Interproton distances were obtained from the initial slopes by using the isolated spin pair approximation.

DFT Calculations. All calculations were carried out using the B3LYP hybrid functional. Full optimizations and transition structure (TS) searches, using the 6-31+G(d) basis set, were carried out with either the Gaussian 98 or Gaussian 03 packages.[18] Analytical frequencies were calculated at the same level of optimization, and the nature of the stationary points was determined in each case according to the appropriate number of negative eigenvalues for the Hessian matrix. Scaled frequencies were not considered since significant errors on the calculated thermodynamical properties are not found at this theoretical level.[19]

Unless stated otherwise, only Gibbs free energies are used for the discussion on the relative stabilities of the considered structures. These energies were obtained using the following correction formula

$$\Delta\Delta G = \Delta\Delta E + \Delta\Delta G_{298} \qquad (3)$$

where $\Delta\Delta E$ is the relative electronic energy and $\Delta\Delta G_{298}$ represents the thermal and entropic corrections at 298 K. All of these values were calculated at the B3LYP/6-31+G(d) level.

Relaxed potential energy surface (PES) scans and intrinsic reaction coordinate (IRC) calculations were carried out at the B3LYP/6-31+G(d) level.

Natural bonding orbital (NBO) analyses were carried out at the B3LYP/6-31+G(d) level using the NBO 3.1 program, as implemented in Gaussian 03. A threshold of 0.01 kcal·mol^{-1} was established for the second-order perturbative estimation of NBO interactions. The orbitals considered were σ (bonding), σ* (antibonding), and n (lone pair). C−C denote bonds between carbons

(18) Frisch, M. J.; Trucks, G. W.; Schlegel, H. B.; Scuseria, G. E.; Robb, M. A.; Cheeseman, J. R.; Zakrzewski, V. G.; Montgomery, J. A., Jr.; Stratmann, R. E.; Burant, J. C.; Dapprich, S.; Millan, J. M.; Daniels, A. D.; Kudin, K. N.; Strain, M. C.; Farkas, O.; Tomasi, J.; Barone, V.; Cossi, M.; Cammi, R.; Mennucci, B.; Pomelli, C.; Adamo, C.; Clifford, S.; Ochterski, J.; Petersson, G. A.; Ayala, P. Y.; Cui, Q.; Morokuma, K.; Malick, D. K.; Rabuck, A. D.; Raghavachari, K.; Foresman, J. B.; Cioslowski, J.; Ortiz, J. V.; Stefanov, B. B.; Liu, G.; Liashenko, A.; Piskorz, P.; Komaroni, I.; Gomperts, R.; Martin, R. L.; Fox, D. J.; Keith, T.; Al-Laham, M. A.; Peng, C. Y.; Nanayakkara, A.; González, C.; Challacombe, M.; Gill, P. M. W.; Johnson, B.; Chen, W.; Replogle, E. S.; Pople, J. A. Gaussian 98, Revisions A.7 and A.11; Gaussian, Inc.: Pittsburgh, PA, 1998.

(19) Bauschlicher, C. W., Jr. *Chem. Phys. Lett.* **1995**, *246*, 40−44.

of the cyclobutane ring. C−R represent bonds between carbons of the cyclobutane ring and the atom of the substituents attached to them; these ones include all the C−H bonds of the cyclobutane ring. N and O refer to nitrogen and oxygen atoms of acetamide and ether groups bonded to the cyclobutane ring.

Hard data on Cartesian coordinates, electronic energies, as well as entropies, enthalpies, Gibbs free energies, and lowest frequencies of the different conformations of all structures considered are available as Supporting Information.

Molecular Modeling. RESP atomic charges[20] in all the compounds simulated in this work were derived by applying the RESP module of the AMBER 6.0 package to the HF/6-31G(d) ESP charges calculated previously with Gaussian 98. All of the simulations were carried out using the SANDER module within AMBER implemented with the general AMBER force field (GAFF). NOE-derived distances were included as time averaged distance constraints. The $<r^{-6}>^{-1/6}$ average for the distances and an exponential decay constant of 400 ps were employed. All the trajectories were carried out using explicit $CHCl_3$ molecules, periodic boundary conditions (PBC), and Ewald sums[21] for the treatment of electrostatic interactions. The SHAKE algorithm[22] for hydrogen atoms and a 1 fs time step were used. Finally, a 9 Å cutoff was applied to Lennard-Jones interactions.

MD-tar simulations were carried out according to the following protocol. First, the cyclobutanes were immersed in a bath of 135−144 $CHCl_3$ molecules. Equilibration of the system was carried out as follows in all cases; as a first step, a short minimization with positional restraints on solute atoms was run to remove any potentially bad contact. The force constant for the positional constraints was 500 kcal·mol^{-1}·Å. A 12.5 ps molecular dynamics calculation was then run at 300 K, maintaining positional restraints on the solute in order to equilibrate the $CHCl_3$ box. For these two steps, a 9 Å cutoff was used for the treatment of the electrostatic interactions. In the next step, the system was equilibrated using the mesh Ewald method. To this end, a short MD simulation (12.5 ps) was run at 300 K, also using the Ewald approach. The system was then subjected to several minimization cycles (each using 1000 steepest descent iterations) gradually reducing positional restraints on the solute from 500 kcal·mol^{-1}·Å to 0. Finally, 4 ns MD trajectories at constant pressure (1 atm) and temperature (300 K) were collected and analyzed using the CARNAL module of AMBER 6.0.

Acknowledgment. We thank the Ministerio de Educación y Ciencia (Project No. CTQ2005-06235/BQU), Gobierno de La Rioja (doctoral fellowship of M.P.-F.), and Universidad de La Rioja (project API-05/B01, doctoral fellowship of G.J.-O.). F.C. and J.H.B. thank the Ministerio de Ciencia y Tecnología for a Ramon y Cajal contract.

Supporting Information Available: NMR data and crystal structure data, as well as computational energy data and coordinates for the structures. This material is available free of charge via the Internet at http://pubs.acs.org.

JO0521955

(20) (a) Bayly, C. I.; Cieplak, P.; Cornell, W. D.; Kollman, P. A. *J. Phys. Chem.* **1993**, *97*, 10269−10280. (b) Cornell, W. D.; Cieplak, P.; Bayly, C. I.; Kollman, P. A. *J. Am. Chem. Soc.* **1993**, *115*, 9620−9631.

(21) Essmann, U.; Perera, L.; Berkowitz, M. L.; Darden, T. A.; Lee, H.; Pedersen, L. G. *J. Chem. Phys.* **1995**, *103*, 8577−8593.

(22) Ryckaert, J. P.; Ciccotti, G.; Berendsen, H. J. C. *J. Comput. Phys.* **1977**, *23*, 327−341.